Fingerprints of Through-Bond and Through-Space Exciton and Charge -Electron Delocalization in Linearly Extended [2.2]Paracyclophanes

Fingerprints of Through-Bond and Through-Space Exciton and π electron delocalization in Linearly Extended [2,2]Paracyclophanes

José Luis Zafra[1], Agustín Molina Ontoria[2], Paula Mayorga Burrezo[1], Mirian Peña-Alvarez[3], Marek Samoc[4], Janusz. Szeremeta[4], Francisco J. Ramírez Aguilar, Ted M. Pappenfus[5], Matthew D. Lovander[5], Christopher J. Droske[5], Luis Echegoyen[6], Juan T. López Navarrete[1], Nazario Martín[2], Juan Casado[1]

[1]*Department of Physical Chemistry, University of Málaga, Campus de Teatinos s/n, Málaga 29071, Spain*

[2]*Department of Organic Chemistry, Faculty of Chemistry, University Complutense of Madrid, 28040 Madrid, Spain.*

[3]*Department of Physical Chemistry, Chemistry Faculty, University Complutense of Madrid, 28040 Madrid, Spain.*

[4]*Advanced Materials Engineering and Modelling Group, Faculty of Chemistry, Wroclaw University of Technology, 50370 Wroclaw, Poland*

[5]*Division of Science and Mathematics, University of Minnesota Morris, MN 56267, USA*

[6]*Department of Chemistry, University of Texas at El Paso, El Paso, TX 79968*, USA

RECEIVED DATE (automatically inserted by publisher);

Abstract. New stilbenoid and thiophenic compounds terminally functionalized with donor-donor, acceptor-acceptor and donor-acceptor moieties and substituting a central [2,2]paracyclophane unit have been prepared and their properties interpreted in terms of through-bond and through space conjugations. A description of the excited state properties based on photophysical data and with focus on the participation of the central [2,2]paracyclophane, or "phane" state, in competition with through-bond conjugation in the arms has been conducted. To this end, one-photon absorption and emission spectroscopy, as a function of temperature, of solvent polarity in solution and of pressure in solid state have been carried out. Furthermore, the analysis of charge delocalization in the face-to-face [2,2]paracyclophane part in the neutral state and in the oxidized species (dications and trications) has been assessed allowing to elucidate the vibrational Raman fingerprint of charge delocalization in these systems. Thus, a complementary approach to "intermolecular" excitation and charge delocalization has been presented in [2,2]paracyclophane model systems by means of the pertinent spectroscopic techniques.

INTRODUCTION

The so-called "*phane state*" of [2.2]paracyclophanes represents an excimer-like state generated by wavefunction delocalization between the two sandwiched benzenes which is promoted by the co-facial through-space coupling of the two aromatic units.[1, 2,3,4,5] Thus [2.2]paracyclophane[6] is a well-defined molecular model for inter-chromophoric exciton and charge delocalization, useful to understand more complex intermolecular phenomena taking place in crystalline and in amorphous solid state organic semiconductors. The [2.2]paracyclophane unit covalently extended with oligoparaphenylene-vinylenes[7,8,9] and oligothiophenes[10,11,12] has been reported as a way to combine through bond (TB) and through space (TS) conjugations in one single molecule (Scheme 1). As a result, structure-property studies on [2.2]paracyclophane based conjugated molecules can provide revealing guidelines to develop novel designs of molecules and polymers with enhanced optoelectronic performance.

In extended [2.2]paracyclophane chromophores, the two relevant electronic communication paths, TB and TS conjugations are placed in a short of perpendicular disposition (Scheme 1) resulting in the formation of complementary states in the sense that they can compete given the nature of their orthogonal arrangement. This highlights a scenario where one can tune the optical and electronic properties from paracyclophane-type to branch-type features with an impact in applications. For instance, this synergistic competition between TB and TS in donor-acceptor extended [2.2]paracyclophane has been exploited in photovoltaic devices, in fact, it has been shown that direct donor-to-acceptor electron transfer is effective in generating the charge separated state (radical anion and cation) but the charge recombination kinetics is slowed down.[5] Given the excimer-like character of the relevant "*phane"* excited state it has been characterized by linear optical[13] methods, by two-photon absorption[8,9,14], fluorescence[1-7] and by nanosecond and microsecond transient absorption spectroscopies[5,15], many of them in the seminal works of Bazan.

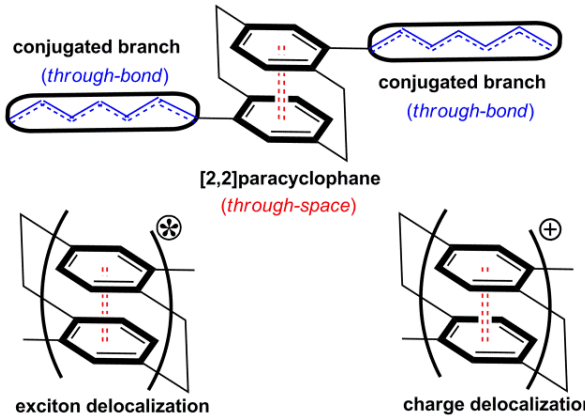

Scheme 1. The [2,2]-paracyclophane unit and the relevant electronic through-bond and through-space electronic effects in conjugated extended systems. Exciton and charge delocalization in the phane state.

Among the many classes of [2.2]paracyclophane substituted with conjugated arms, two different concepts have been mainly studied: i) those with "linear" shape, or pseudo-para-derivatives, where the branches are aligned in the same direction (these branches can be identical or having a donor-acceptor

structure[16,17,18]); and ii) those with "banana" shape, or pseudo-ortho-derivatives where the branches are disposed in 2D directions.[1,3,8] Since the interaction between TB and TS conjugation channels govern the relevant optical properties, we will study several cases of linearly substituted [2.2]paracyclophane derivatives (all compiled in Scheme 2) where the conjugated arms are: i) phenylene-vinylene (PV, stilbene) substituted at the terminal positions with electron acceptor groups of variable electron-withdrawing strength, or acceptor-acceptor dyads; ii) the same derivatives where the acceptors are substituted by bisphenyl amino groups, or donor-donor dyads; iii) the [2.2]paracyclophane PV core substituted with a donor group at one side and an acceptor in the other, or donor acceptor-dyads; and iv) donor-donor dyads where the stilbenoid branches are replaced by thiophenes.

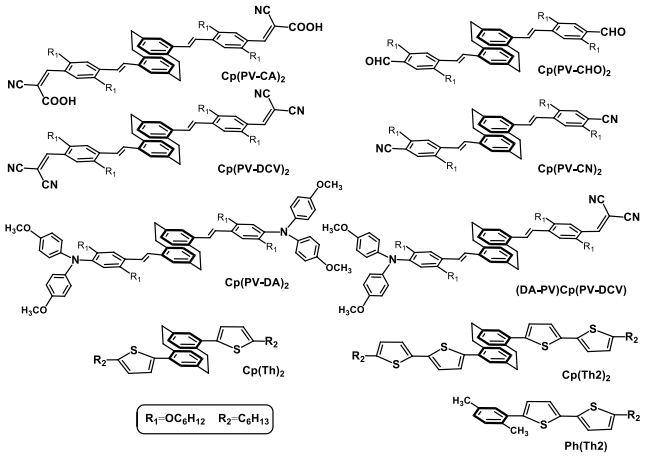

Scheme 2 Chemical structures and nomenclature of the [2,2]paracyclophnes (Cp) studied in this work.

The objective of the study is to focus on those properties governed by the [2.2]paracyclophane or *phane* unit for which we will pay special attention to: i) those excited states which disclose excitonic delocalization in the neutral molecules, and ii) to the ground electronic state of the oxidized species disclosing charge delocalization between the parallel benzenes. A variety of linear absorption and photoluminescence methods (solvato–, thermo–chromism, pressure-dependent properties and two-photon absorption) will be explored in the case of the excited state analysis. To address charge delocalization in the ground electronic state, the vibrational Raman spectra in different oxidized species (dications and radical trications) will be discussed. Quantum chemical calculations will support and help to understand the spectroscopic data.

Experimental and Theoretical Details.

1. Synthesis. The preparation of the symmetrically functionalized donor-donor, acceptor-acceptor [2.2]paracyclophane derivatives was carried out by stepwise syntheses following well-established protocols under inert atmosphere. Starting dialdehyde Cp(PV-CHO)$_2$ was obtained as previously described.[19] Similarly, the syntheses of the dicyano derivative Cp(PV-CN)$_2$ and diphenylamine derivative Cp(PV-DA)$_2$ were carried out by two-fold Heck Pd-catalyzed reaction between 4,16-divinyl[2.2]paracyclophane and 4-iodobenzonitrile and/or 4-iodo-N,N-bis(4-methoxyphenyl)aniline in good yields (67-75%). On the other hand, malononitrile and cyanoacetic acid were convalently connected to the dialdehyde Cp(PV-CHO)$_2$ by two-fold Knoevenagel condensation affording Cp(PV-DCV)$_2$ and Cp(PV-CA)$_2$ in 89% and 91% yields, respectively. The synthesis of asymmetrically substituted precursors bearing donor and acceptor moieties was performed by two consecutive Heck reactions to afford compound **6** (see Supporting information for details, Section S1). Finally, (DA-PV)Cp(PV-DCV) was obtained by a Knoevenagel condesation between malononitre and monoaldehyde **6** in 83% yield. The aforementioned new compounds were spectroscopically characterized by using the standard techniques (FTIR, ^{1}H NMR, ^{13}C NMR and HR-MS, in Supporting Information, Section S1). As representative spectroscopic features, all the compounds showed the signal corresponding to the ethylene bridges as three broad multiplets, integrating for 2:1:1, in the range of 2.8-3.6 ppm in the ^{1}H NMR spectra. The chemical structure of all new compounds were ascertained by HR-MS. Previously, Collard and coworkers reported the use of Stille coupling to produce donor-donor compounds with thiophenes in place of stillbenoid branches around the paracyclophane core.[10] According to the authors, however, this coupling method provided analytically impure products in low yield. We now report the use of Suzuki coupling to produce similar compounds with high purity (according to combustion analyses) in moderate to good yield as shown in Scheme 3. Addition of hexyl-capped thienyl or bithienyl boronic esters to 4,16-dibromo[2.2]paracyclophane produced Cp(Th)$_2$ and Cp(Th$_2$)$_2$ in yields of 79% and 41% respectively. The model compound, Ph(Th$_2$) (Scheme 1) was prepared in a similar manner using 2-bromo-p-xylene in place of the dibromoparacyclophane. Structures of these new molecules were confirmed with ^{1}H and ^{13}C NMR (see Supporting Information, Section S2).

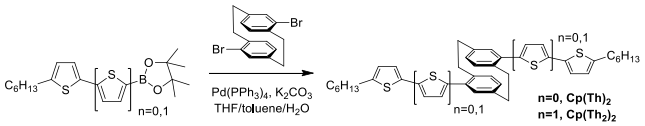

Scheme 3. Preparation of thiophene-based donor-donor materials.

2. Absorption and emission measurements. UV-vis absorption and Fluorescence spectra are recorded in a FLS920P spectrofluorometer from Edinburgh Analytical Instruments equipped with a pulsed xenon flash-lamp using the time correlated single photon counting (TCSPC) operation mode. UV-Vis-NIR spectra are measured in a Cary 3000 spectrophotomer.

3. Raman spectroscopy. The Raman spectra were recorded in resonance conditions either by using the 1064 or 785 nm excitations. The 1064 nm FT–Raman spectra were obtained with an FT–Raman accessory kit (FRA/106–S) of a Bruker Equinox 55 FT–IR interferometer. A continuous–wave Nd–YAG laser working at 1064 nm was employed for excitation. A germanium detector operating at liquid nitrogen temperature was used. Raman scattering radiation was collected in a back–scattering configuration with a standard spectral resolution of 4 cm^{-1}. 1000–3000 scans were averaged for each spectrum. Raman spectra with the 785 nm excitation were collected by using the 1×1 camera of a Bruker Senterra Raman microscope by averaging spectra during 50 minutes with a resolution of 3–5 cm^{-1}. A CCD camera operating at –50 ºC was used.

4. Third-order nonlinear optical characterization. The third-order nonlinear properties were investigated using the Z-scan technique. This technique allows to simultaneously measure both the real Re(γ) and imaginary Im(γ) part of the cubic hyperpolarizability that are responsible for nonlinear refraction and nonlinear absorption, respectively. The nonlinear absorption data can also be presented as the two-photon absorption cross section σ_2. The measurements were performed in the wavelength range from 560 nm to 1000 nm using laser pulses from a Quantronix Palitra-FS optical parametric amplifier (OPA), pumped with 130 fs, 800 nm

pulses at 1 kHz repetition rate from a Quantronix Integra-C Ti:Sapphire regenerative amplifier. Open and closed-aperture Z-scan traces were recorded simultaneously by a pair of photodetectors, one of which was obscured by 1 mm aperture. A detailed description of the experimental procedure can be found elsewhere.[20] The results were analyzed using the equations derived by Sheik-Bahae et al. [21]Samples of the [2.2] paracyclophane derivatives were prepared as 1% w/w chloroform solutions in 1 mm path length glass cuvettes.

5. Pressure dependent mesurements.

Emmision high pressure experiments were conducted in a sapphire anvil cell (SAC)[i]with a diameter culet of 360 μm and a gold gasket. As pressure calibrant the PL shift of the anvils [ii,iii] using the sapphire R1 and R2 bands. [iv] No pressure transmitting medium to discard interactions between pressure-transmitting media and the samples. An air-cooled ILT argon ion laser operated at 488.0 nm is used to excite both the fluorescence . Emission measurements were conducted using a AvaSpec-2048-2 spectrometer with a 1200l/mm grating.

Raman pressure dependent were conducted with the same anvils configuration using the shift of diamond chips as the pressure calibrant.[v] Raman measurements were performed using an air-cooled argon ion laser, a Spectra-Physics solid state laser, operating at 532.0, nm. The device is equipped with a 10x Mitutoyo long working distance objective coupled to a 10x Navitar zoom system and focused onto the slit of an ISA HR460 monochromator with a grating of 600 grooves mm^{-1} and a liquid nitrogen cooled CCD detector (ISA CCD3000, 1024−256 pixels). Spectra were measured with a spectral resolution of about 2−3 cm^{-1} and calibrated with a standard neon emission lamp. For PL and Raman measurements the SAC is mounted on a xyz stage, which allows us to move the sample with an accuracy of 1 μm. The typical sampling area was about 1−2 μm in diameter.

6. Theoretical calculations. Quantum-chemical calculations were done in the framework of the density functional theory[22] as implemented in the Gaussian´09 package.[23] Simulations were performed in the gas-phase. The B3LYP[24] and exchange-correlational functional and the 6-31G**[25] basis set were used in all calculations. Theoretical frequencies were scaled down by a uniform scale factor of 0.96.[26] The unrestricted-B3LYP/6-31G** approach was used for the open-shell radical trication and dications. To simulate the open-shell ground-state structures of the dications, we used the broken-symmetry option with the key guess=mix keyword also with the unrestricted wavefunctions at the (U)B3LYP level.

RESULTS AND DISCUSSION

A. Acceptor-Acceptor Dyads.

A.1 Absorption spectra and orbital description. Figure 1 displays the spectra of the acceptor-acceptor dyads in tetrahydrofurane at 298 K.

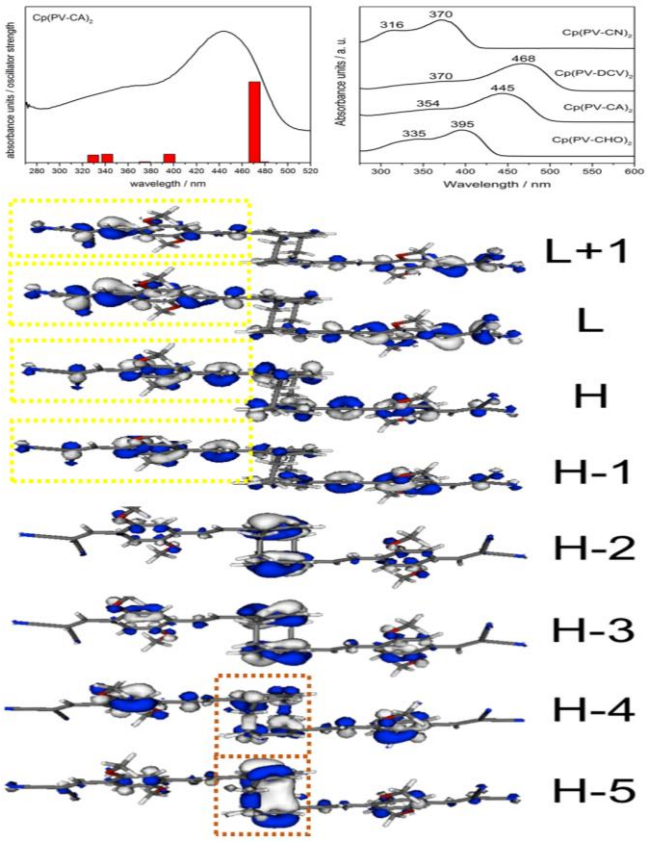

Figure 1. Top) Absorption spectrum of $Cp(PV\text{-}CA)_2$ together with the TD/DFT theoretical excitations (red bars) and absorption spectra of the four compounds in THF at 298K. Bottom) Frontier molecular orbitals topologies of $Cp(PV\text{-}CA)_2$. Yellow and marron boxes highlight the main orbital π−distribution.

The most intense absorption of $Cp(PV\text{-}CA)_2$ is at 445 nm which at the TD/DFT/6-31G** level (see Figure S1 for the theoretical spectra) corresponds with the $S_0 \rightarrow S_3$ excitation at 471 nm (oscillator strength, *f*= 2.07) described as the sum of two one-electron promotions between the H-1→L and H→L orbitals. These principal orbitals in Figure 1 (Figure S2 and Table S1) are centered in the branches with the two benzenes of the PV units participating in the TB conjugation in the arms. Instead, between the two benzenes of the paracyclophane unit no interactions are noticeable. There is a medium intensity band at 354 nm in the experimental spectrum predicted as the $S_0 \rightarrow S_7$ excitation calculated at 396 nm (*f*=0.22) and arising from multi-electron promotions between the H-4→L and H-2→L+1 orbitals. The third experimental band at 330 nm is related with the $S_0 \rightarrow S_{11}$ excitation calculated at 342 nm (*f*=0.21) and due to an H-5→L promotion (the theoretical band at 330 nm with f=0.19 might also contribute to this 354 nm experimental feature). Interestingly these two last excitations involve orbitals where inter-ring cofacial wavefunction delocalization within the [2.2]paracyclophane, or TS conjugation, is feasible, in particular in the H-4 and H-5 orbitals.

Calculations on the model compound consisting only of the isolated arm (PV-CA unit), or donor-acceptor TB conjugated compound, show that the lowest energy lying electronic transition is due to the $S_0 \rightarrow S_1$ excitation which is mostly associated with a HOMO→LUMO promotion (see Figure S3 and Table S2). In this PV-CA structure, the HOMO wavefunction is mainly placed on the donor PV unit whereas the LUMO is mostly on the cyano-carboxylic-vinylene moiety. Thus, this excitation promotes an electron density shift on the molecule or CT character. In contrast, in the $Cp(PV\text{-}CA)_2$ dyad, the lowest energy excitations (i.e., the

$S_0 \rightarrow S_1$ and $S_0 \rightarrow S_2$ are forbidden transitions (oscillator strength, f=0) and are consequently inactive in the one-photon absorption spectrum. This means that in $Cp(PV\text{-}CA)_2$ a significant blue-shift of the strongest observed UV-Vis band regarding that of the individual donor-acceptor arm is observed (from $S_0 \rightarrow S_1$ in the PV-CA arm to the $S_0 \rightarrow S_3$ in the $Cp(PV\text{-}CA)_2$ dyad).

In the four compounds, the strongest absorption bands move to the red 445→468 and 354→370 nm on $Cp(PV\text{-}CA)_2$→ $Cp(PV\text{-}DCV)_2$ given the strengthening of the acceptor character upon replacing the carboxylic group by another cyano. The main electronic absorption bands of the UV-Vis spectra of the cyano and aldehyde substituted dyads [i.e., $Cp(PV\text{-}CHO)_2$ and $Cp(PV\text{-}CN)_2$] display their bands considerably blue shifted regarding the other two Cp derivatives in agreement with the diminished electron-withdrawing strength of their terminal groups.

A.2 Emission fluorescence spectra. The photophysical properties reported for [2.2]paracyclophane-based conjugated molecules have been interpreted in terms of the relative energy location of the "phane" TS excimer-like "inter-chromophoric" state regarding the "local-arms" TB "intra-chromophoric" state in Scheme 4.

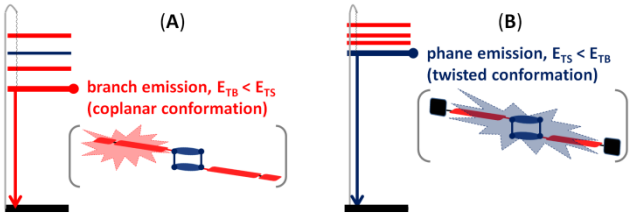

Scheme 4. Relative disposition of the relevant excited states (TB states on the branches; blue: TS state in the [2,2]paracyclophane unit). A) Emission from the TB arms state. B) Emission from the TICT state.

For long conjugated arms, the energy of the local TB state (E_{TB}, Scheme 4) is lower than that of the "phane" TS state (E_{TS}, Scheme 4) and either absorptions as emissions are dominated by the former excited state. Conversely, in the case of short conjugated arms ($E_{TB} > E_{TS}$), the photophysical properties are dictated by the delocalized TS "phane" state. According to our description above, the molecular orbitals containing the TS interaction (H-4, H-5) are contributing to excited states high in energy compared with the states contributed by the TB orbitals (H, H-1, etc.). On the other hand, it is well known that, in despite of in short conjugated arms the E_{TB} state is destabilized regarding the E_{TS}, the inclusion of acceptor moieties on them enables the decrease of the E_{TB} energy and thus the situation of these donor-acceptor short branches becomes similar to the situation of [2.2]paracyclophanes substituted with large conjugated platforms.

Figure 2A displays the excitation and emission spectra of $Cp(PV\text{-}CA)_2$ and $Cp(PV\text{-}DCV)_2$ in a polar solvent such as N,N-dimethylformamide. Excitation of the strongest absorption band at 420 nm of $Cp(PV\text{-}CA)_2$ gives rise to a broad featureless emission at 480 nm, however by exciting at 350 nm, dual emission is recorded which consists of a higher energy emission component with vibronic structure between 400-430 nm which is followed by a second emission at 480 nm identical to the one described by exciting the lowest absorption band. In the first experiment we promote the $S_0 \rightarrow S_3$ excitation which is a TB excited state placed in the conjugated arms which relaxes by internal conversion to the lowest energy S_1 excited state, also confined in the conjugated arms, from which emits light (case A in Scheme 4). This $S_1 \rightarrow S_0$ emission is weak (the $S_0 \rightarrow S_1$ absorption is inactive) and featureless given its charge transfer character (HOMO→LUMO). By exciting the "phane" state at 360 nm, we observe another high energy vibronically resolved band which might be ascribed to an emission from a mixed state involving the [2.2]paracyclophane and extended over the conjugated arms which explains the vibronic activity (the acceptor groups do not participate, case B in Scheme 4). Since the TB and TS states are orthogonally decoupled, this mixed excited state can either emit or being depopulated by internal conversion to the S_1 charge transfer excited state responsible for the second or lowest energy emission.

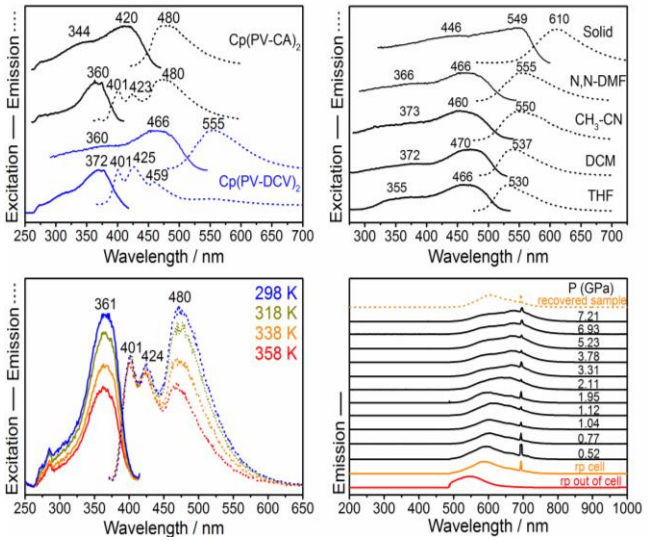

Figure 2. A) Excitation/emission Spectra of $Cp(PV\text{-}CA)_2$ and $Cp(PV\text{-}DCV)_2$ in N,N-DMF at 298K. B) Excitation/emission spectra of $Cp(PV\text{-}DCV)_2$ recorded in solid state (red) and in different solvents (black). C) Excitation/emission spectra of $Cp(PV\text{-}CA)_2$ as a function of temperature. D) Emission Spectra of $Cp(PV\text{-}DCV)_2$ in solid state as a function of applied pressure when excited with 488 nm.(Peaks around 693-695 nm correspond to the fluorescence peaks of the sapphire anvils

In order to justify why the electronic contributions of the acceptor groups are removed in this mixed excited state, we can invoke the situation found in conjugated donor-acceptor dyes with the appearance of twisted intramolecular charge transfer (TICT) states which fully decouple the donor-acceptor interaction.[27] This might likely be our case in the N,N-dimethylformamide polar solvent. A very similar situation is found for $Cp(PV\text{-}DCV)_2$ where exciting the "phane" state produces a vibronically resolved emission at the same wavelength as the $Cp(PV\text{-}CA)_2$ corroborating that it emerges from the common [2.2]paracyclophane phenylene-vinylene spacer (TICT state). In this case, the lowest energy charge transfer emission is resolved at 555 nm, red-shifted relative to the analogue emission at 480 nm in $Cp(PV\text{-}CA)_2$.

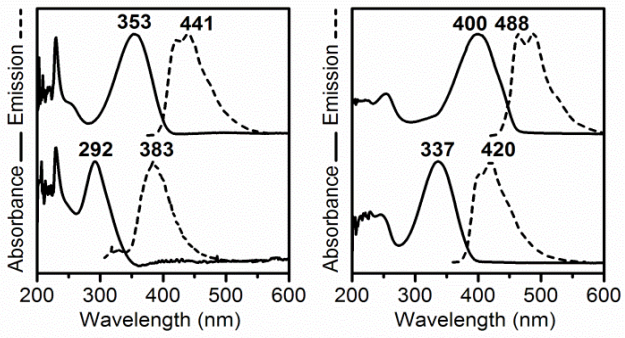

Figure 3. A) UV-Vis absorption and emission spectra in dichloromethane of $Cp(Th)_2$ (Left-bottom), $Cp(Th2)_2$ (Left-top), Ph-Th2 (Right-bottom) and dimethylquaterthiophene (Right-top)

To further understand the excited state distribution resulting from the [2,2]paracyclophane insertion, two new compounds where thiophene units replace the stilbene branches have been prepared. The two new compounds possess one ($Cp(Th)_2$ or two ($Cp(Th2)_2$) thiophenes in each branch terminated with hexyl groups. In Figure 3 the absorption and emission spectra of the two compounds together with the reference (i.e., the isolated arm) compound Ph-Th2 are shown. The absorption maximum is at 292 nm in $Cp(Th)_2$ and red-shifts to 353 nm in $Cp(Th2)_2$. These spectra are in excellent agreement with methyl terminated homologues previously published by Collard.[10] The exclusive effect of the insertion of the [2,2]paracyclophane, or of the TS conjugation, is seen by comparing the Ph-Th2 reference compound with $Cp(Th2)_2$ and dimethylquaterthiophene (i.e., the parent compound without the central [2,2]paracyclophane unit). The reference compound displays an absorption maximum at 337 nm whereas that of dimethylquaterthiophene and $Cp(Th2)_2$ display maxima at 400 nm and 353 nm respectively. These data reveal the effect of the inclusion of the [2,2]paracyclophane unit and concomitantly of TS conjugation. This influence is also seen in the wavelength maxima of the emission spectra as these are detected at 383 nm in $Cp(Th)_2$, at 420 nm in the Ph-Th_2 arm, at 488 nm in dimethylquaterthiophene, and at 441 nm in $Cp(Th2)_2$. The noticeable aspect of the emission spectra of $Cp(Th2)_2$ and Ph-Th_2 is the vibronic structure, while the emission spectrum of $Cp(Th)_2$ is featureless clearly indicating the participation of the "phane" excited state in the emission of $Cp(Th)_2$ while this is deactivated in the branch centered emission of $Cp(Th_2\text{-}CH_3)_2$, such described in the stilbenoid [2,2]paracyclophanes.

A.3 Solvent, temperature and pressure absorption and fluorescence spectra of Cp(PV-CA)₂ and Cp(PV-DCV)₂. To further confirm these interpretations, we have carried out the photophysical measurements in an apolar solvent like dichloromethane (Figure 2B) where no double emission is observed. The weak polar character of this solvent deactivates the TICT effect by which the acceptors remain coupled with the conjugated PV unit in the TB path. Furthermore, we have carried out fluorescence emission spectra as a function of the temperature in Figure 2C for $Cp(PV\text{-}CA)_2$. We observe that by increasing the temperature the lowest-lying energy CT emission declines in intensity in favor of the mixed "phane" TICT state, an effect that we might explain in terms of increased conformational mobility at high temperatures around the single bond connecting the phenylene-vinylene unit with the acceptor which directly promotes the TICT effect and its vibronically resolved emission.

Solvent and temperature measurements modify the acceptor molecular environment, hence, in order to get further insights about the central "phane" unit, a pressure dependent emission experiment in solid state has been carried out in Figure 2D.[28] With pressure we expect to modify the face-to-face interaction in the [2,2]paracyclophane core by slightly reducing the inter-benzene distance. Owing to the large sensitivity of the energy of the excimer-like "phane" state to this inter-annular distance, a modification of the emission features is expected. In the solid state at ambient pressure, by exciting the 488 nm excimer-like "phane" absorption, no double emission is observed, instead the TB emission of the branches appears further displaced to the red at 610 nm regarding the solution spectrum. Moreover, at high pressure up to 1.95 GPa, we find that the TB charge transfer emission at 610 nm develops a low energy feature at 680 nm that becomes the most intense emission component at 7.0 GPa. Please, poned menos espectros y marcad esto, ahora no se ve bien!

For all pressures analyzed at room temperature, the 610 and 680 nm components coexist whereas the original spectrum is recovered after pressure release. These results can be accounted for by two facts: i) The formation of a TICT excited state with "phane" emission is highly impeded in the solid due to largely restricted conformational freedom. Conformational constraint further provokes reduced structural reorganization after excitation and thus smaller Stokes shifts and the appearance of re-absorption phenomena, mostly on the 0-0 component. This will allow the detection of 0-1/0-2/etc/ hot vibronic components such as the 680 band; and ii) The application of pressure might produce a compression of the [2,2]paracyclophane unit increasing the π–π cofacial benzene interaction that stabilizes the mixed excimer-like "phane" which might thus appear at lower energies partially overlapped with the low energy TB band and , as a result, contributing to explain the 600-700 nm rich band profile of this emission under pressure. In the ESI podríamos comparer con la emission medida para el CP(th2) y el $Cp(PV\text{-}CN)_2$ donde estos cambios que aquí se mencionan solo se ven para el *Cp(PV-DCV)₂*

A.4 Two-photon absorption properties. We have measured the two-photon absorption cross-section (σ_2(GM)) for the four stilbenoid compounds by means of the Z-scan technique using a tunable femtosecond laser system. Table 1 summarizes the data from the third-order nonlinear measurements at wavelengths corresponding to σ_2 peaks and Figure 4 displays the two-photon absorption cross-section spectra.

Table 1. Third-order NLO data determined with the Z-scan technique.

Sample	λ_{max} [nm]	Re(γ) [10^{36}esu]	Im(γ) [10^{-36}esu]	σ_2 [GM]	σ_2/M [GM mol/g]
$Cp(PV\text{-}CHO)_2$	625	-230	200	82	0.094
	850	62	160	36	0.041
$Cp(PV\text{-}CA)_2$	675	-1080	730	255	0.254
	825	-670	1050	247	0.246
$Cp(PV\text{-}DCV)_2$	650	-670	610	233	0.241
	825	-240	1440	340	0.352
$Cp(PV\text{-}CN)_2$	600	-530	102	45	0.052
	900	-72	74	15	0.017

For better comparison of the data between the compounds having different molecular masses, we also present the merit factor which is two-photon absorption cross-section divided by the molar mass (σ_2/M). This also allows for comparison between various types of nonlinear materials (small molecules, polymers, branched dendrimers or nanoparticles).[29]

The discussion of the linear absorption/emission properties highlights a scenario where the TB and TS states exited states are distinctively affected by several environmental and molecular changes. The existence of two identical donor acceptor branches connected through the [2,2]paracyclophane unit gives rise to a opposite arrangement of the local dipole moments on each branch provoking the appearance of excitations which might be prone to two-photon absorption activity.[8,9,14] Compounds $Cp(PV\text{-}CA)_2$ and $Cp(PV\text{-}DCV)_2$ disclose the most noticeable σ_2(GM) TPA values which are much higher than those of $Cp(PV\text{-}CHO)_2$ and $Cp(PV\text{-}CN)_2$ given their smaller π–spaces and electron-withdrawing strengths (both weaken the charge transfer character). Two main TPA peaks are observed in the spectra at 825 and 680 nm. The

TPA band maximum at 825 nm, which is accompanied by a higher wavelength peak around 880 nm, can be associated with the $S_0 \rightarrow S_2$ and $S_0 \rightarrow S_1$ excitations respectively theoretically predicted at 472/480 nm (944/960 nm).. There are two other two less intense TPA bands around 680 nm which might be correlated with the one-photon silent excitations, $S_0 \rightarrow S_4$, $S_0 \rightarrow S_5$ and $S_0 \rightarrow S_6$, predicted theoretically at 446, 404 and 399 nm respectively.

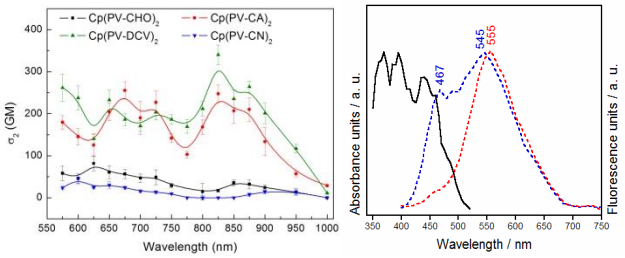

Figure 4. Left: two-photon absorption spectra recorded with the Z-scan techniques. Right: two-photon induced up-conversion fluorescence analysis for compound $Cp(PV\text{-}DCV)_2$ in N,N-DMF.

In order to complete the TPA study in connection with the distributions of excited states, we have conducted two-photon induced up-conversion fluorescence analysis for compound $Cp(PV\text{-}DCV)_2$ as a representative example. The spectra are shown in Figure 4. We notice that by exciting at the longest wavelength (900 nm, TPA state at 450 nm) we observed only one fluorescence emission peak at 555 nm in line with the excitation of the lowest energy lying TPA active excited states of the branches ($S_0 \rightarrow S_1$ and $S_0 \rightarrow S_2$). By exciting at shorter wavelengths, between 850 and 750 nm, we observed the two fluorescent peaks with maxima at 467 and 545 nm, respectively, in agreement with the excitation of the higher energy TPA active excited state ($S_0 \rightarrow S_4/S_5/S_6$) with increasing participation of "phane" state. Figure 4 also shows the TPA excitation spectra which corroborate our assignments with the relevant TPA absorptions placed between the one-photon absorption bands.

A.5 Raman spectroscopic properties. The discussion above mainly concerns the energy position and activity of the excited states arising from TB and TS conjugation, a critical aspect to correctly design the channel for energy migration in molecules. In order to complete the characterization of [2,2] paracyclophanes molecules, we now address the conjugational properties in the ground electronic state by means of Raman spectroscopy, a vibrational technique that provides the vibrational Raman frequencies associated to those vibrational normal modes involved in the C=C/C-C conjugational paths. Figure 5 displays the Raman spectra of the acceptor-acceptor dyads and in Supporting Information (Figure. S4) we provide the theoretical spectrum of $Cp(PV\text{-}CA)_2$ which allows us to assign their bands in terms of vibrational normal modes, also in Figure S4.

ω	1626 cm^{-1}	1602 cm^{-1}	1587 cm^{-1}	1552 cm^{-1}	1562 cm^{-1}
Assigment	$\nu_{int}(C=C)$	$\nu_{TB}(CC)$	$\nu_{1pCp}(CC)$	$\nu_{2pCp}(CC)$	$\nu_{ext}(C=C)$

The band at 1626 cm^{-1} corresponds to a C=C stretching vibration of the internal vinylene bond [i.e., $\nu_{int}(C=C)$] which connects to the [2,2]paracyclophane; that at 1602 cm^{-1} arises from a CC stretching vibration of the PV benzene rings (i.e., $\nu_{TB}(CC)$, in the TB conjugation path), whereas the band at 1587 cm^{-1} corresponds to a CC stretching mode of the benzenes in the [2,2]paracyclophane segment [i.e., $\nu_{1pCp}(CC)$]. A second band exclusive of the [2,2]paracyclophane fragment is at 1552 cm^{-1} arising from an analogue CC stretching mode [i.e., $\nu_{2pCp}(CC)$]. The most intense Raman band is at 1562 cm^{-1} and emerges from a C=C stretching vibration of the external double bond [i.e., $\nu_{ext}(C=C)$] connected with the acceptors units. This assignment agrees with that proposed for the [2,2]paracyclophane compound which describes their relevant CC stretching modes in this region at 1599 and 1559 cm^{-1} respectively.[28]

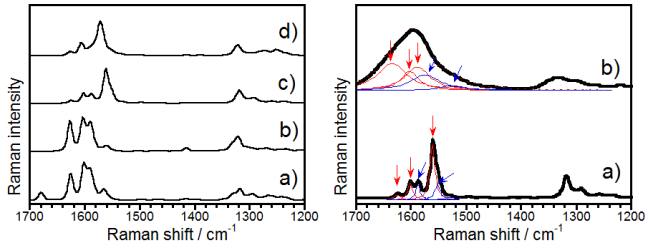

Figure 5. Left: FT-Raman spectra of the four compounds in solid state: a) $Cp(PV\text{-}CHO)_2$, b) $Cp(PV\text{-}CN)_2$, c) $Cp(PV\text{-}DCV)_2$, d) $Cp(PV\text{-}CA)_2$. Right: Raman spectra of a) $Cp(PV\text{-}DCV)_2$ in solid state at room pressure and b) at 8 GPa using 532 nm as excitation line (to enable the comparison the fluorescence background has been subtracted). Lorentzian deconvolutions are shown in colors.

	$Cp(PV\text{-}CN)_2$	$Cp(PV\text{-}DCV)_2$	$Cp(PV\text{-}CA)_2$	$Cp(PV\text{-}CHO)_2$
$\nu_{1pCp}(CC)$	1590 cm^{-1}	1587 cm^{-1}	1587 cm^{-1}	1592 cm^{-1}
$\nu_{2pCp}(CC)$	1559 cm^{-1}	1552 cm^{-1}	1552 cm^{-1}	1565 cm^{-1}
$\nu_{TB}(CC)$	1604 cm^{-1}	1602 cm^{-1}	1606 cm^{-1}	1602 cm^{-1}
$\nu_{int}(C=C)$	1627 cm^{-1}	1625 cm^{-1}	1626 cm^{-1}	1626 cm^{-1}

With this description of the vibrational Raman spectrum in terms of ground electronic state frequencies, we are in disposition of inspecting their evolution in the different series. The two $\nu_{pCp}(CC)$ bands are at 1590/1559 cm^{-1} in $Cp(PV\text{-}CN)_2$, 1587/1552 cm^{-1} in $Cp(PV\text{-}DCV)_2$, 1588/1554 cm^{-1} in $Cp(PV\text{-}CA)_2$ and 1592/1565 cm^{-1} in $Cp(PV\text{-}CHO)_2$ indicate affectation of the [2,2]paracyclophane Raman bands. In general, for the vibrational modes associated with CC stretching modes of the aromatic benzenes a frequency downshift reveals the transformation of the benzoaromatic-like structure into a benzoquinoidal-like one. Therefore comparing $Cp(PV\text{-}CHO)_2$ and $Cp(PV\text{-}DCV)_2$, we detect the larger $\nu_{pCp}(CC)$ frequency downshift resulting of the stronger electron-withdrawing effect of the dicyanovinyls compared with the aldehyde derivative imparted along the TB path. For the Raman frequency behavior related to the $\nu_{TB}(CC)$ benzene and the $\nu_{int}(C=C)$ vinylene bands, these appear at 1602/1625 cm^{-1} in $Cp(PV\text{-}DCV)_2$, 1606/1626 cm^{-1} in $Cp(PV\text{-}CA)_2$, 1604/1627 cm^{-1} in $Cp(PV\text{-}CN)_2$ and 1602/1626 cm^{-1} for $Cp(PV\text{-}CHO)_2$ showing again changes towards a more TB conjugated situation in the cases with stronger acceptors. From these data, changes associated with TS conjugation cannot be deduced.

Micro-Raman spectroscopy allows us to follow the frequency changes under pressure in solid state. We have conducted pressure dependent Raman experiments of $Cp(PV\text{-}DCV)_2$ shown in Figure 5 which pursuits to selectively modify the TS conjugation in the [2,2]paracyclophane core. The first noticeable effect of pressure in the Raman spectra is the overall spectral broadening which is a consequence of the increment of intermolecular interactions (with pressure we are moving from the absolute minimum along the repulsive branch of the ground electronic state potential energy surface). As a result of this, frequencies experience a general up-shift. According to the presence of five bands in the spectrum of $Cp(PV\text{-}DCV)_2$ at room pressure (RP), we have de-convoluted the broad Raman feature at 1530-1600 cm^{-1} into five Lorentzian components (Figure 5, fit of 0.99) which emerge at 1632 cm^{-1}

(i.e., related with the ν_{int}(C=C) at 1626 cm^{-1} at RP), at 1604 cm^{-1} (i.e., related with the ν_{TB}(CC) at 1602 cm^{-1} at RP), at 1588 cm^{-1} (i.e., related with the ν_{ext}(C=C) at 1562 cm^{-1} at RP), at 1573 cm^{-1} (i.e., related with the ν_{1pCp}(CC) at 1587 cm^{-1} at RP) and finally at 1525 cm^{-1} (i.e., related with the ν_{2pCp}(CC) at 1552 cm^{-1} at RP). Two clear behaviors are observed: i) that of the bands at 1632/1604/1588 cm^{-1} depict a small to moderate upshift regarding frequencies at RP; and ii) that of the bands at 1573/1525 cm^{-1} downshift with increasing compression. The three first bands are due to the substituent arms and the upshift is caused by the increment of intermolecular interactions. However, the second pair of bands own to the [2,2]paracyclophane units contrarily downshift upon compression. Li. et. al [vi] observed that the compression of the pure [2.2] paracyclophane unit induced the reversible closure of the inner cavity. So it is clear that application of pressure on the paracyclophane squishes the structure provoking a decrease of the interbenzene distance. However, the difference between compressing the unsubsittued [2.2] paracyclophane core and the Cp(PV-DCV)$_2$ is that while in the former the ν_{2pCp}(CC) and ν_{1pCp}(CC) upshift with compression, in the Cp(PV-DCV)$_2$ these downshift due to the induced TS conjugation enabled by the arms. TS conjugation might displace π–electron density from the benzene ring to the inter-annular region at the origin of the Raman downshifts.

B. Donor-Donor Dyads.

B.1 Ground electronic state properties. In the donor-donor derivatives, the vinyl-acceptor groups have been substituted by donor amino-phenyl moieties. The insertion of the nitrogens incorporate new excited states originated from transitions involving the lone electron pair, or n→π* excitations, by which the analysis of the emission properties in connection with the TB or TS features is not straightforward. Conversely, these donor-donor molecules, allow the analysis of the conjugational TB/TS properties in the context of charge delocalization in the oxidized species.

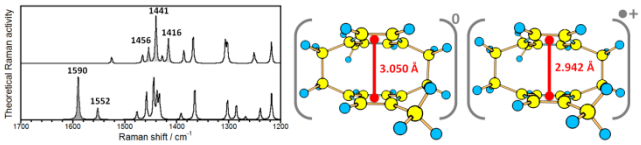

Figure 6. (U)B3LYP/6-31G* theoretical Raman spectra of the dimethyl [2,2]paracyclophane unit in the neutral (bottom) and radical cation (top) states together with the optimized geometries.

Figure 6 shows the theoretical Raman spectra of the [2,2]paracyclophane unit alone where the two arms in the studied model compound have been replaced by methyls. The Raman spectrum of the neutral model displays the two characteristic Raman bands at 1590 and 1552 cm^{-1} already discussed as exclusively emerging from this part. In the radical cation state the theoretical Raman spectrum is featured by a strong band at 1441 cm^{-1} which is accompanied by medium intensity bands at 1456 and 1416 cm^{-1} which represent the vibrational fingerprint of a structure (phane state in Scheme 1) where the positive charge is delocalized between the two benzenes and, as a result, displays a inter-benzene distance smaller than in the neutral case, 3.050 →2.942 Å, according to calculations.

Diaminoaryl stilbene paracylcophanes (Cp(PV-DA)$_2$, donor-donor dyads) have been prepared (see Supporting Information for synthetic details). Amino compounds are well known to act as excellent electron donors moieties and, complementarily to the acceptor-acceptors dyads, allow to addressing the paracyclophane effect when positive charge delocalization takes place. In Figure 7 we show the UV-Vis-NIR spectra obtained during the *in situ* electrochemical (see Supporting information for the electrochemical characterization, Section S4) and chemical oxidations of Cp(PV-DA)$_2$. Interestingly, at potentials in the two-electron oxidation window, we solely record a spectrum that consists of the appearance of three main bands at 531(573), 705 and 1062 nm, a spectroscopic pattern typical of open-shell radical cations, in this case a bis(radical cation) species (i.e., dication). This dicationic species can be viewed as an acceptor-acceptor dyad, in fact, the structured band at 500-570 nm can be correlated with that at 468 nm in Cp(PV-DCV)$_2$. Thus the two remaining Vis-NIR bands are due to the open-shell nature of the bis(radical cation). Further oxidation of this species gives rise to a clear distinctive band at 755 nm that co-exists with the bands of the dication and that could result from a third-oxidized species, or radical trication.

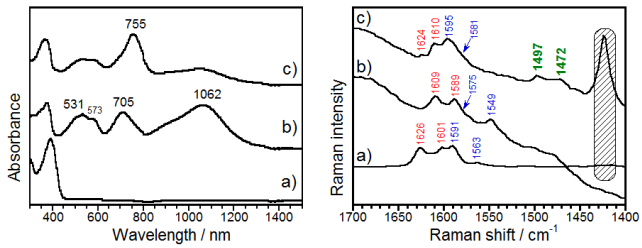

Figure 7. UV-Vis-NIR (left) and Raman (right) spectra of the neutral (a), dication (b) and radical trication (c) of Cp(PV-DA)$_2$.

Figure 7 displays the Raman spectra of Cp(PV-DA)$_2$ donor-donor dyads in the three relevant oxidation states. The spectrum of the neutral species features the presence of four bands due to the ν_{int}(C=C) at 1626 cm^{-1}, the ν_{TB}(CC) benzene at 1601 cm^{-1} and the two bands due to the ν_{pCp}(CC) at 1591/1563 cm^{-1}. Oxidation of neutral Cp(PV-DA)$_2$ gives rise to the direct formation of the dication with a Raman spectrum that evidences a general downshift of the frequencies of the four Raman bands due to the weakening of the vinylene bond, and the quinoidization of the benzenes. Further oxidation of this dication gives way to the radical trication which, in contrast with the behavior of the neutral→dication, displays a general upshift of the frequency bands passing from the dication to the triply charged molecule. In addition two new medium intensity bands appear at 1497/1472 cm^{-1}.

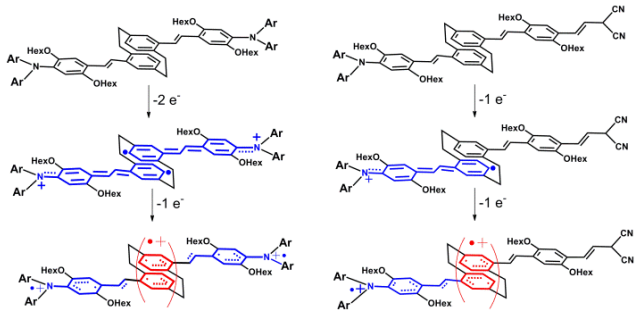

Scheme 5. Resonant forms stabilizing the charged species of Cp(PV-DA)$_2$ (left) and of PV-DA)Cp(PV-DCV) (right).

In Scheme 5 the main resonant forms associated with the different oxidized species and that could justify the Raman frequency changes are represented. In the dication of Cp(PV-DA)$_2$, the structural alteration spreads over the whole branch forming quinoidal structures in the benzene and a transformation

of the vinylene towards a more simple character bond. However, in the trication the charge is extracted mainly from the central paracyclophane while the existing positive charges of the dication are pushed towards the nitrogen somehow getting rid of the quinoidal structure. Therefore the new Raman bands of the radical trication at 1497/1472 cm^{-1} might be related with the formation of a phane state with charge delocalization within the two co-facial benzenes. These Raman bands are in good agreement with the Raman spectrum predicted for the radical cation of the dimethyl [2,2]paracyclophane unit which supports the presence of charge delocalization in the radical trication of Cp(PV-DA)$_2$ and of the participation of the phane state in the stabilization of the charge.

C. Donor-Acceptor Dyads.

We have also prepared the bis-aryl amino donor and dicyano-vinyl acceptor substituted paracyclophane compound, (PV-DA)Cp(PV-DCV), which shows a one-electron oxidation at +0.45 V (see Supporting information for the electrochemical characterization, Section S4). Figure 8 shows the electrochemical UV-Vis-NIR spectra of (PV-DA)Cp(PV-DCV) where the disappearance of the neutral bands gives way to the spectrum of the radical cation characterized by the three bands 534/585, 710 and 1047 nm which nicely correlate with the bands of the bis(radical cation) of Cp(PV-DA)$_2$. In both cases the central paracyclophane unit is surrounded by two acceptor moieties, the two radical cations in [Cp(PV-DA)$_2$]$^{(\bullet+)2}$ and one radical cation and a dicyano vinylene branch in $^{(\bullet+)}$(PV-DA)Cp(PV-DCV). Posterior oxidation of $^{(\bullet+)}$(PV-DA)Cp(PV-DCV) allows the formation of the dication species thanks to the participation of the paracyclophane unit which contributes to the stabilization of the high oxidation state. The spectrum is composed by only one band at 757 nm which nicely correlates with the band at 755 nm assigned in the radical trication of Cp(PV-DA)$_2$ which further reveals the participation of the central common paracyclophane in the stabilization of the two related species, the dication and radical trication.

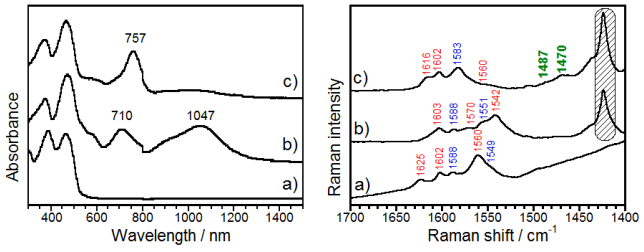

Figure 8. UV-Vis-NIR (left) and Raman (right) spectra of the neutral (a), radical cation (b) and dication (c) of (PV-DA)Cp(PV-DCV).

Figure 8 also displays the Raman spectra of these oxidized species of (PV-DA)Cp(PV-DCV). Again the Raman spectrum contains the Raman bands associated to the ν_{int}(C=C)/ν_{ext}(C=C) at 1625/1560 cm^{-1}, the 1602 cm^{-1} band of the benzene ν_{TB}(CC) and the ν_{pCp}(CC) features at 1588/1549 cm^{-1}. Oxidation, such as in the case of Cp(PV-DA)$_2$, produces an overall frequency downshift which is now ascribed to the formation of the radical cation placed and delocalized on the bis(aryl)amino stilbene unit producing the quinoidization of the benzene and the transformation of the vinylene. Further oxidation of this radical cation to the dication reproduces a similar behavior to that found from the dication to the radical trication of Cp(PV-DA)$_2$ consistent with an overall frequency upshift of these bands due to the mitigation of the quinoidal structure characteristic of the radical cation. The presence of an acceptor branch on one side and of a radical cation on the other forces the second electron extraction to be placed at the paracyclophane unit such as shown in Scheme 5. The new bands on this dication at 1487/1470 cm^{-1} are therefore the characteristic vibrational signature of the paracyclophane state such as described in the radical trication of Cp(PV-DA) by comparing with dimethyl [2,2]paracylcophane radical cation.

Interestingly, in the Raman experiment of Cp(PV-DCV)$_2$ in neutral state with pressure discussed in section A.5, a significant frequency downshift was detected for the [2,2]paracyclophane bands upon application of pressure (1587 →1573 cm^{-1} and 1552 →1525 cm^{-1}), a behavior which is also consistent with the strong downshifts from ≈1550 cm^{-1} to 1470 cm^{-1} for the new bands observed in the radical trication and dication of Cp(PV-DA)$_2$ and (PV-DA)Cp(PV-DCV) respectively. In the former case the charge delocalization between the two sandwiched benzene is provoked by pressure and in the oxidized species the driving force is the stabilization of the positive charge by delocalization as well. Obviously the latter effect results in much stronger alteration of the inter-benzene distance and therefore the greater impact on the vibrational frequencies.

CONCLUSIONS

Intermolecular exciton and charge delocalization is an important topic in organic electronics as it is at the origin of the energy and charge transport in the semiconductor substrates. In order to better understand these complex processes, molecules with well-defined and precise structures and conformations are required in order to establish feasible structure-properties relationships. Here we choose the [2,2]paracylcophane unit which has a face-to-face blocked conformation of two benzenes separated by ≈3 Å and therefore mimicking the effect of through-space delocalization. We study several new [2,2]paracylcophane derivatives by enlarging linearly the central unit with stilbene moieties further substituted with donor, acceptors in several formats, and also thiophene derivatives replacing the stilbenoid bridges.

The detection of dual fluorescence allows us to get insights of the excited state ordering which is responsible of the different emission properties measured. We described how the enlargement of conjugation on the linear arms push emissions far from the [2,2]paracylcophane while limited conjugation of the arms is the efficient way for the sandwiched structure to be involved in the emissions. We analyze the excited states of by using one- and two-photon absorption properties which allows to characterize the bright and dark excited states with and without [2,2]paracylcophane participation.

In a different spectroscopic approach by using Raman spectroscopy for the study of the ground electronic state properties, the vibrational Raman fingerprints of charge delocalization in the benzene-benzene interface have been described. By conducting pressure dependent Raman measurements, we partially modify the inter-benzene distance thus permitting enhanced through space conjugation. In addition, the localization of a positive charge between the two benzenes allows this to be delocalized in the through-space region. Interestingly, the increase of TB conjugation produces characteristic frequency downshifts of the most intense Raman bands.

In summary, dual fluorescence and Raman shifts provide the fingerprints for through-space conjugation and allows us to comprehensively explore the excited state and ground electronic state properties when through-bond and through space conjugations compete for the exciton or for the injected charge. Very recently (porphyrin)donor-(fullerene)acceptor molecules connected by di-stilbenoid [2,2]paracyclophane units have been described in which direct porphyrin→C60 electron transfer efficiently occurs by means of to the participation of the "phane" state which helps the energy migration or internal conversion of the initial excitation in the donor towards the acceptor permitting final charge separation. However, this charge separated state is formed on the two branches disconnected because of the absence of "phane" state or though-bond localized states such as described in this work. This exemplifies the relevance of a good understanding of the excited state properties and distribution in order to afford efficient molecular systems for organic electronic applications.

Acknowledgements. The work at the University of Málaga was supported by MINECO through project reference CTQ2012-33733 and by the Junta de Andalucía through research project P09-FQM-4708. T.M.P. acknowledges University of Minnesota, Morris (UMM) Faculty Research Enhancement Funds supported by the University of Minnesota Office of the Vice President for Research. We thank Mercedes Taravillo and Valent'in Garc'ia Baonza (UCM) for the support provided during the high pressure measurements. MPA thanks to the CTQ2015-67755-C2-1-R project.

Supporting Information. Synthetic procedures, chemical characterizations, details of the quantum chemical calculations, and a complete list of authors for some references. This information is available free of charge via the Internet at http://pubs.acs.org

References.

(1) Bartholomew, G. P.; Bazan, G.C., *Acc. Chem. Res.*, **2001**, 34, 30-39.

(2) Bazan, G.C.; Oldham, W.J.; Lachicotte, R. J.; Tretiak, S.; Chernyak, V.; Mukamel, S., *J. Am. Chem. Soc.*, **1998**, 120, 9188-9204.

(3) Hong, J. W.; Woo, H. Y. ; Liu, B. ; Bazan, G.C., *J. Am. Chem. Soc.*, **2005**, 127, 7435-7443.

(4) Mukhopadhyay, S.; Jagtap, S. P. ; Coropceanu, V. ; Brédas, J. L. ; Collard, D. M., *Angew. Chem. Int. Ed.*, **2012**, 124, 11797-11800. Elacqua, E.; Bucar, D. K.; Skvortsova, Y. ; Baltrusaitis, J.; Geng, M.L. ; MacGillivray, L. R., *Org. Lett.*, **2009**, 11, 5106-5109.

(5) Molina-Ontoria, A.; Wielopolski, M. ; Gebhardt, J. ; Gouloumis, A. ; Clark, T. ; Guldi, D.M. ; Martin, N., *J. Am. Chem. Soc.*, **2011**, 133, 2370-2373.

(6) Vogtle, F. *Cyclophane Chemistry*; J. Wiley & Sons: Chichester, England, 1993. *Modern Cyclophane Chemistry*; Gleiter, R., Hopf, H., Eds.; Wiley-VCH: Weinheim, Germany, 2004.

(7) Ruseckas, A.; Namdas, E. B. ; Lee, J.Y. ; Mukamel, S. ; Wang, S. ; Bazan, G.C. ; Sundstrom, V., *J. Phys. Chem. A*, **2003**, 107, 8029-8034.

(8) Woo, H. Y.; Hong, J. W. ; Liu, B. ; Mikhailovsky, A. ; Korystov, D. ; Bazan, G.C., *J. Am. Chem. Soc.*, **2005**, 127, 820-821.

(9) Bartholomew, G. P.; Rumi, M. ; Pond, S. J.K. ; Perry, J. W. ; Tretiak, S. ; Bazan, G.C., *J. Am. Chem. Soc.*, **2004**, 126, 11529-11542. Zyss, J.; Ledoux, I. ; Volkov, S.; Chernyak, V. ; Mukamel, S. ; Bartholomew, G. P. ; Bazan, G.C., *J. Am. Chem. Soc.*, **2000**, 122, 11956-11962.

(10) Salhi, F.; Lee, B. ; Metz, C. ; Bottomley, L. A. ; Collard, D. M., *Org. Lett.*, **2002**, 4, 3195-3198.

(11) Salhi, F. ; Collard, D. M., *Adv. Mater.*, **2003**, 15, 81-85.

(12) Jagtap, S. P. ; Mukhopadhyay, S. ; Coropceanu, V. ; Brizius, G. L. ; Brédas, J. L. ; Collard, D. M., *J. Am. Chem. Soc.*, **2012**, 134, 7176-7185. Knoblock, K. M.; Silvestri, C. J. ; Collard, D. M., *J. Am. Chem. Soc.*, **2006**, 128, 13680-1368.

(13) Canuto, S.; Zerner, M.C., *J. Am. Chem. Soc.*, **1990**, 112, 2114-2120.

(14) Fuke, K.; Nagakura, S. ; Kobayashi, T., *Chem. Phys. Lett.*, **1975**, 31, 205-207.

(15) Kaiser, C.; Schmiedel, A. ; Holzapfel, M.; Lambert, C., *J. Phys. Chem. C*, **2012**, 116, 15265-15280.

(16) Leng, W. ; Grunden, J. ; Bartholomew, G. P. ; Bazan, G.C. ; Myers Kelley, A., *J. Phys. Chem. A*, **2004**, 108, 10050-10059.

(17) Moran, A. M. ; Bartholomew, G. P. ; Bazan, G.C. ; Myers Kelley, A., *J. Phys. Chem. A*, **2002**, 106, 4928-4937.

(18) Nelsen, S. F. ; Konradsson, A. E. ; Telo, J.P., *J. Am. Chem. Soc.*, **2005**, 127, 920-925.

(19) Referencias síntesis Nazario-Agus.

(20) Szeremeta, J.; Kolkowski, R.; Nyk, M.; Samoc, M., *J. Phys. Chem. C*, **2013**, 117, 26197-26203.

(21) Sheik-bahae, M.; Said, A. A.; Van Stryland, E. W. Op. Lett. 1989, 14, 955-957.

(22) Stephens, P. J.; Devlin, F. J.; Chabalowski, C. F.; Frisch, M. J. *J. Phys. Chem.* **1994,** *98*, 11623.

(23) Gaussian 09, Revision D.01, Frisch, M. J. *et al.* Gaussian, Inc., Wallingford CT, (2009).

(24) Becke, A. D. *J. Chem. Phys.* **1993**, *98*, 1372.

(25) Francl, M. M.; Pietro, W. J.; Hehre, W. J.; Binkley, J. S.; Gordon, M. S.; Defrees, D. J.; Pople, J. A. *J. Chem. Phys*. **1982**, *77*, 3654.

(26) Scott, A. P.; Radom, L. *J. Phys. Chem*. **1996**, *100*, 16502.

(27) Grabowski, Z. R.; Rotkiewicz K.; Rettig, W., *Chem. Rev*., **2003**, 103, 3899–4032. Sasaki, S.; Drummen, G.P. C.; Konishiac, G., *J. Mater. Chem C*., **2016**, 4, 2731-2743.

(28) Li, W.; Sui, Z. ; Liu, H. ; Zhang, Z. ; Liu, H., *J. Phys. Chem. C*, **2014**, 118, 16028-16034.

(29) Samoc; M.; Matczyszyn, K.; Nyk, M.; Olesiak-Banska, J.; Wawrzynczyk, D.; Hanczyc, P.; Szeremeta, J.; Wiel gus, M.; Gordel, M.; Mazur, L.; Kolkowski, R.; Straszak, B.; C ifuentes, M. P.; Humphrey, M. G. Proc. SPIE, *Organic Photonic Materials and Devices XIV*, 82580V, 2012.

To format double-column figures, schemes, charts, and tables, use the following instructions:

Place the insertion point where you want to change the number of columns
From the **Insert** menu, choose **Break**
Under **Sections**, choose **Continuous**
Make sure the insertion point is in the new section. From the **Format** menu, choose **Columns**
In the **Number of Columns** box, type **1**
Choose the **OK** button

Now your page is set up so that figures, schemes, charts, and tables can span two columns. These must appear at the top of the page. Be sure to add another section break after the table and change it back to two columns with a spacing of 0.33 in.

Table 1. Example of a Double-Column Table

Column 1	Column 2	Column 3	Column 4	Column 5	Column 6	Column 7	Column 8

Authors are required to submit a graphic entry for the Table of Contents (TOC) that, in conjunction with the manuscript title, should give the reader a representative idea of one of the following: A key structure, reaction, equation, concept, or theorem, etc., that is discussed in the manuscript. Upon reduction, the TOC graphic should be no wider than 4.72 in. (12 cm) and no taller than 1.81 in. (4.6 cm).

Insert Table of Contents artwork here

ABSTRACT FOR WEB PUBLICATION (Word Style “BD_Abstract”). Authors are required to submit a concise, self-contained, one-paragraph abstract for Web publication.

[i] Del Corro, E.; González, J; Taravillo, M.; Flahaut, E.; Baonza, V. G. *Nano Lett.* **2008**,8, 2215-2218 ().

[ii] P. Loubeyre, F. Occelli, R. LeToullec, *Nature*, 2002, **416**, 613-617.

[iii] B. J. Baer, M. E. Chang, W. J. Evans, *J. Appl. Phys*., 2008, **104**, 034504.

[iv] Piermarini GJ, Block S, Barnett JD, Forman JA.J. Appl. Phys. 1975; 46: 2774.. Syassen, K.(2008). High Pressure Research, 2008, 28:2,75 — 126

[v] Baonza, V. G.; Taravillo, M.; Arencibia, A.; Cáceres , M.; Núñez, J.; *J. Raman Spectrosc.* **2003**, 34, 264-270.

[vi] Li, W.; Sui, Z.; Liu, J.; Zhang, Z.; Liu, H.; *J. Phys. Chem. C*, 2014, **118**, 16028-16034.